IMPROVED BILATERAL FILTERING SCHEME FOR NOISE REMOVAL IN COLOR IMAGES

Krystyna Malik, Bogdan Smolka
Polish-Japanese Institute of Information Technology
Koszykowa 86, 02-008 Warsaw, Poland
krystyna.malik@polsl.pl, smolka@ieee.org

ABSTRACT

In this paper a new approach to the problem of noise removal in color images is presented. The proposed filtering design is a modification of the bilateral denosing scheme, which takes into account the similarity between color pixels and their spatial distance. However, instead of direct calculation of the dissimilarity measure, the cost of a connection through a digital path joining the central pixel of the filtering window with the remaining pixels is determined. The filter output, like in the standard bilateral filter, is calculated as a weighted average of the pixels surrounding the center of the filtering window, and the weights are functions of the minimal connection costs. Experimental results prove that the introduced design yields significantly better results than the bilateral filter in the case of color images contaminated by strong mixed Gaussian and impulsive noise.

KEYWORDS

Color image enhancement, impulsive noise removal

1 INTRODUCTION

Visual information processing is increasingly becoming widespread as multimedia becomes common in everyday life. With the expanding use of color images in various multimedia applications and the proliferation of color capturing and display units, the interest in color image enhancement is rapidly growing.

Quite often, color images are corrupted by various types of noise introduced by malfunctioning sensors in the image formation pipeline, electronic instability of the image signal, faulty memory locations in hardware, aging of the storage material, transmission errors and electromagnetic interferences due to natural or man-made sources [1–4].

Noise reduction is one of the most frequently performed image processing operation, as the enhancement of images or video streams degraded by noise, is indispensable to facilitate subsequent image processing steps.

In this work we focus on the restoration of color images corrupted by mixed Gaussian and impulsive noise. The reduction of such kind of noise is quite a challenging task, as the techniques capable of reducing efficiently the Gaussian noise, fail in the presence of impulses and the methods suited for the removal of impulsive noise are mostly ineffective when restoring images distorted by other noise types [5–7].

In recent years the problem of the suppression of mixed noise in color images attracted much research interest [8–10]. The most widely used filtering designs are based on the concept of the *Vector Median Filter* (VMF), whose output is computed using the concept of *vector ordering* of a set of pixels from the filtering window.

The vector ordering scheme is defined through the sorting of the *cumulated distances* from a given pixel to all other pixels from the filtering window. Then the scalar sums of distances are sorted and the associated vectors can be correspondingly ordered [3, 11, 12]. The vector median filter is very effective at reducing impulsive noise, however its efficiency is decreased when the image is distorted by Gaussian noise, and therefore in such a case the

VMF is usually combined with other noise suppression designs.

Many noise reducing designs are based on the concept of adaptive weighted averaging, where the weights are assigned to the pixels from a filtering window according to some rules which downweight the influence of outlying observations [13–15]. An efficient scheme proposed in [16, 17] divides the pixels of the filtering window into two sets. The first one consists of the pixels similar to the central pixel of the local window and the other one is composed of those pixels, which diverge greatly from the central pixel. The output is computed as a weighted average of the peer-group members.

Similar concept is utilized by the technique proposed in [18], which calculates the distances between the central pixel in a local window and its neighbors. If the number of pixels classified as close to the central pixel is higher than a predefined threshold, then the pixel is treated as uncorrupted, otherwise it is replaced by a vector median of all pixels from the window or an average of the uncorrupted pixels. In [19] the peer-group members were found using a technique based on the evaluation of the statistical properties of a sorted sequence of accumulated distances used for the calculation of the vector median. The peer-group concept has been also successfully extended to the fuzzy context, so that the proposed technique is able to remove mixed noise by combining a statistical method for impulse noise detection and a replacement scheme utilizing an averaging operation aimed at smoothing out the Gaussian noise component [20, 21].

One of the major problems of many noise reducing methods is the blurring of edges. To overcome this undesired effect the *Anisotropic Diffusion* (AD) technique has been proposed [22], whose aim is to remove the noise component in homogeneous areas, while inhibiting smoothing across the edges. This task is accomplished through the introduction of a nonlinear diffusion scheme, which smoothes the image in directions parallel to edges and prevents blurring across object boundaries. In this way the AD technique is capable of reducing the image noise while simultaneously enhancing its edges.

Since the introduction of the AD method which was intended for gray scale image denoising, the extension to vector valued images was elaborated [23, 24] and a variety of techniques inspired by the anisotropic diffusion based approach have been proposed.

An efficient method of image denoising called *Non-Local Means* (NLM) was proposed in [25, 26]. This method is based on a non-local averaging of the image pixels in such a way that the new pixel value of the restored image is estimated as a weighted average of the pixels, whose local neighborhood is similar to the local neighborhood of the pixel which is currently being processed. The NLM filter is extremely efficient when restoring images corrupted by Gaussian noise, but fails in the presence of distortions introduced by impulsive noise.

The remainder of the paper is organized as follows. In Section 2, we describe the concept of the standard Bilateral Filter and in the next Section we introduce its modification which enables to effectively cope with strong mixed Gaussian and impulsive noise. In Section 4 we evaluate the efficiency of the proposed filtering design and compare it with the bilateral scheme and some other denoising techniques briefly described in the Introduction. Section 5 concludes this paper with some remarks and directions for future research.

2 Bilateral Filter

Another powerful nonlinear noise reducing filtering design, whose aim is to smooth images while preserving their edges, called *Bilateral Filter* (BF) was proposed in [27] and discussed in [28–30].

In this method, the intensity value of the pixel $\boldsymbol{x}$ is being replaced by a weighted average of the intensities of all other pixels belonging to the filtering window $W_{\boldsymbol{x}}$ centered at $\boldsymbol{x}$. The weight function depends on the spatial distance between the central pixel and other pixels of $W_{\boldsymbol{x}}$ as well as on the difference of their intensities. The BF output $J(\boldsymbol{x})$ at image domain location $\boldsymbol{x}$ is defined as

$$J(\boldsymbol{x}) = \frac{1}{Z} \sum_{\boldsymbol{y} \in \mathcal{N}_{\boldsymbol{x}}} w(\boldsymbol{x}, \boldsymbol{y}) I(\boldsymbol{y}), \; Z = \sum_{\boldsymbol{y} \in \mathcal{N}_{\boldsymbol{x}}} w(\boldsymbol{x}, \boldsymbol{y}), \quad (1)$$

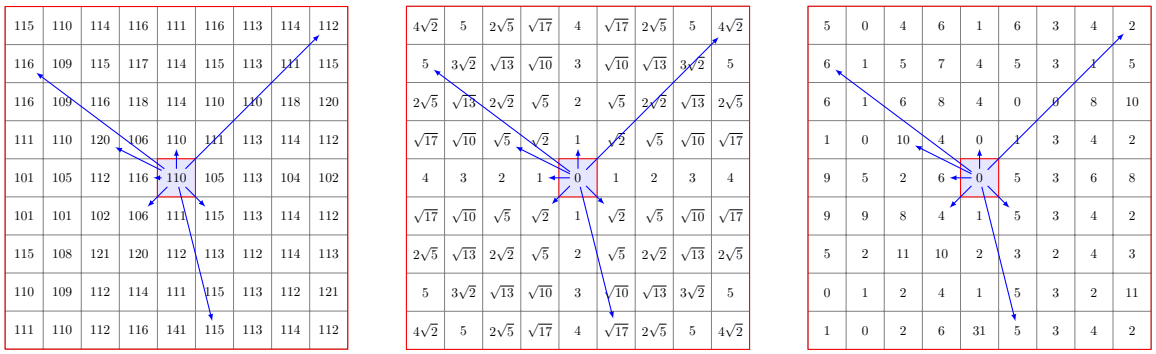

(a) filtering window (b) spatial distances (c) intensity differences

Figure 1: Illustration of the bilateral filter construction.

where $\mathcal{N}_{\boldsymbol{x}}$ is the set of pixels included in $W_{\boldsymbol{x}}$ so that $W_{\boldsymbol{x}} = \{\mathcal{N}_{\boldsymbol{x}} + \boldsymbol{x}\}$, $w(\boldsymbol{x}, \boldsymbol{y})$ is the weight assigned to pixel at location $\boldsymbol{y}$. The weight assigned to pixel at $\boldsymbol{y} \in \mathcal{N}_{\boldsymbol{x}}$ is defined as

$$w(\boldsymbol{x}, \boldsymbol{y}) = w_S(\boldsymbol{x}, \boldsymbol{y}) \cdot w_I(\boldsymbol{x}, \boldsymbol{y}). \tag{2}$$

This weight is a result of multiplication of two components

$$w_S(\boldsymbol{x}, \boldsymbol{y}) = \exp\left(-\frac{\|\boldsymbol{x} - \boldsymbol{y}\|^2}{2\sigma_S^2}\right), \tag{3}$$

$$w_I(\boldsymbol{x}, \boldsymbol{y}) = \exp\left(-\frac{|I(\boldsymbol{x}) - I(\boldsymbol{y})|^2}{2\sigma_I^2}\right), \tag{4}$$

where $\|\cdot\|$ denotes the Euclidean distance between pixels $\boldsymbol{x}$ and $\boldsymbol{y}$, σ_S and σ_I are tuning parameters in the *spatial* and *intensity* domains respectively.

The w_S weighting function decreases with the Euclidean distance, so that the pixels which are far away from the center of the processing window have low influence on the weighted averaged expressed by (1). The w_I weighting function is a decreasing function of the absolute difference of pixel intensities. Thus, the weight w_I operating in the intensity domain reduces the influence of pixels whose intensities significantly differ from that of the central pixel, which ensures the preservation of sharp image edges and preservation of image details.

Figure 1 explains the construction of the bilateral filter. It depicts an exemplary filtering window (a), the array of Euclidean distances between the central pixel and all other pixels of the window (b) and the array of the absolute differences of intensities (c).

For color images, the difference of intensities is replaced by the distance between color pixels in the RGB color space. Using the Euclidean norm, we obtain

$$\|\boldsymbol{I}(\boldsymbol{x}) - \boldsymbol{I}(\boldsymbol{y})\|^2 = \sum_{k=1}^{3} \left(I_k(\boldsymbol{x}) - I_k(\boldsymbol{y})\right)^2, \tag{5}$$

where $\|\boldsymbol{I}(\boldsymbol{x}) - \boldsymbol{I}(\boldsymbol{y})\|$ is the distance between the RGB vectors at $\boldsymbol{x}$ and $\boldsymbol{y}$ and the index represents the k-th color channel, (Red, Green or Blue).

Therefore, for color image the scheme given in (4) can be extended and the weight w_I can be expressed as

$$w_I(\boldsymbol{x}, \boldsymbol{y}) = \exp\left(-\frac{\|\boldsymbol{I}(\boldsymbol{x}) - \boldsymbol{I}(\boldsymbol{y})\|^2}{2\sigma_I^2}\right). \tag{6}$$

The bilateral filter is a highly efficient noise reducing scheme, however it has severe problems to remove the pixels introduced by impulsive noise process. Assuming that the central pixel of the local filtering window is an impulse and some of the pixels in the window are also injected by the noise and possess similar intensities or colors as the central pixel, then the weights expressed by (6) are relatively high, which leads to the preservation of the corrupted pixel.

This undesired effect is illustrated by the situation depicted in Fig. 2. If in the close vicinity of a noisy pixel, another similar pixels corrupted by noise are present, then while calculating the new pixel value, the noisy pixel will be included

with large weights and as a result the impulses will be preserved. In the depicted example, the filtering window contains pixels whose intensities are equal to 128 and some bright impulses with intensities equal to 255. The weights (depicted near the arrows) assigned to white pixels are large and the weights of gray pixels are very close to 0 for $\sigma_I = 20$ and $\sigma_S = 2$. As a result the white impulse in the center of the filtering window will be preserved as only the bright pixels will be taken for the weighted average, which is the output of the bilateral filter.

Therefore, in this paper we propose a modification of the bilateral filter, which alleviates the described above drawback.

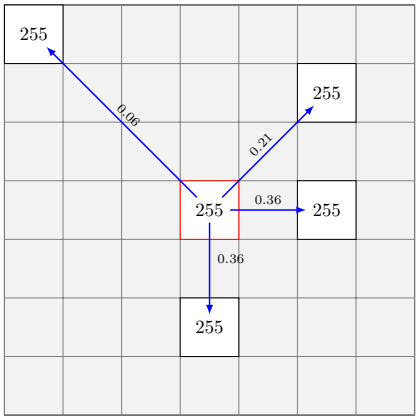

Figure 2: Illustration of the BF inability to suppress impulsive noise.

3 Modified Bilateral Filter

The concept of the proposed modification of the bilateral filter is based on assigning the pixels from the filtering window $W_{\boldsymbol{x}}$ a minimum connection cost of a digital path which joins them with the central pixel $\boldsymbol{x}$. In this way, each pixel is connected with the central pixel through a digital path with minimum cost function value. The connection cost is used to calculate a weight assigned to each pixel from $W_{\boldsymbol{x}}$ and the filter output is the weighted average of the pixels in $\mathcal{N}_{\boldsymbol{x}}$.

For the calculation of the weights we treat the local filtering window as a directed graph, whose nodes are the pixels and whose arcs are determined by the 8-adjacency relation, (Fig. 3a). The

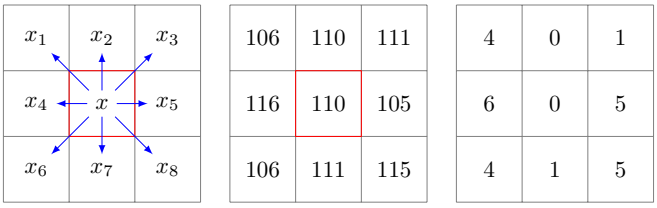

(a) (b) (c)

Figure 3: Adjacency relation (a), pixel intensities (b) and their absolute differences with respect to the central pixel (c).

cost of a path in such a graph is the sum of connection costs between the adjacent pixels forming a path and the connection cost (arc cost) is assumed to be a function of the absolute difference of their intensity.

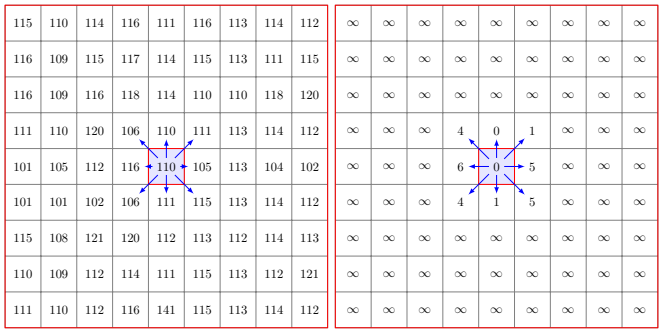

(a) filtering window (b) crossing costs

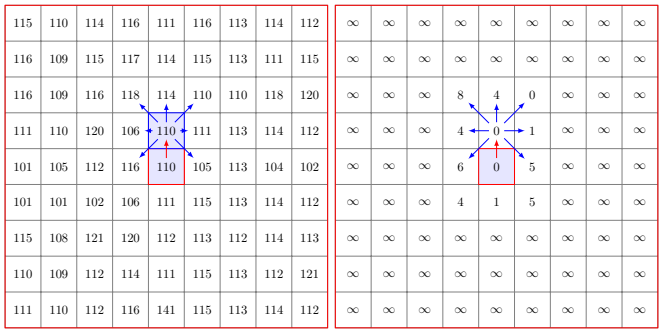

(c) first pixel is visited (d) updated costs

Figure 4: Initial steps of the creation of minimum connection paths.

For finding the minimum cost paths we apply the Dijkstra algorithm [31], where the graph weights are simply the absolute differences between adjacent pixel intensities. Thus, a minimum connection cost of a pixel at position $\boldsymbol{y}$ is defined

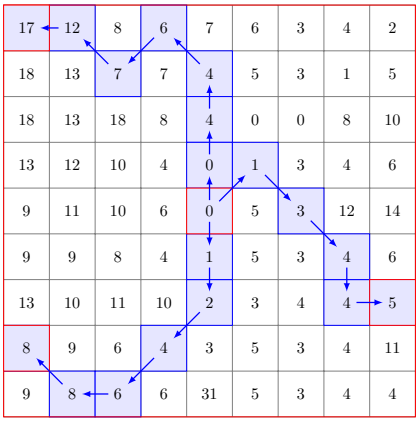

Figure 5: Connection costs with some exemplary minimum paths.

as a minimum sum of absolute differences between the pixels constituting a digital path connecting this pixel with the central pixel of the filtering window centered at $\boldsymbol{x}$.

Figure 3 illustrates the application of the Dijkstra algorithm for the evaluation of the connection cost. The central pixel of W is denoted as $\boldsymbol{x}$, and the neighboring pixels as $\boldsymbol{x}_k$, $(k = 1, \ldots, 8)$ and the connection cost $c(\boldsymbol{x}, \boldsymbol{x}_k)$ between adjacent pixels is

$$c(\boldsymbol{x}, \boldsymbol{x}_k) = |I(\boldsymbol{x}) - I(\boldsymbol{x}_k)|. \tag{7}$$

For the computation of the optimal paths connecting the pixels with the central pixel $\boldsymbol{x}$ a cost array C is created. Initially $C(\boldsymbol{x}) = 0$ and $C(\boldsymbol{y}) = \infty$, for all pixels $\boldsymbol{y}$ belonging to $\mathcal{N}_{\boldsymbol{x}}$, which indicates that the pixels were not yet assigned a connection cost value. At the beginning, the cost of the crossing between the central pixel and its neighbors is calculated (Fig. 4). Afterwards the Dijkstra algorithm creates the paths of the lowest total cost and assigns the optimal costs to the pixels from the filtering window. Every pixel of the window is visited and whenever a path with a lower cost is found, the corresponding value of the cost array C is updated. Finally, this array includes the lowest costs and determines the minimum cost path connecting a given pixel with the center pixel as shown in Fig. 5. In this way, as every pixel of the filtering window is connected by a simple path of minimum total cost with the central pixel $\boldsymbol{x}$ of W, the considered graph can be treated as a tree with the root at $\boldsymbol{x}$ [32].

The connection costs can be treated as similarity measures between the pixel $\boldsymbol{x}$ and and the remaining pixels of the processing window. In this way, the proposed filtering scheme is simply a weighted average of the pixels $\boldsymbol{y} \in \mathcal{N}_{\boldsymbol{x}}$. The weights are defined as

$$\tilde{w}(\boldsymbol{x}, \boldsymbol{y}) = \exp\left(-\frac{C(\boldsymbol{x}, \boldsymbol{y})^2}{h^2}\right), \tag{8}$$

where h is a tuning parameter and $C(\boldsymbol{x}, \boldsymbol{y})$ is a cost function of the minimum path connecting $\boldsymbol{x}$ and $\boldsymbol{y}$.

The cost function assigned to $\boldsymbol{y}$ is the minimum total cost of the connection between $\boldsymbol{x}$ and $\boldsymbol{y}$

$$C(\boldsymbol{x}, \boldsymbol{y}) = \sum_{j=1}^{m} |I(\boldsymbol{x}_j) - I(\boldsymbol{x}_{j-1})|, \tag{9}$$

where $\boldsymbol{x}_0 = \boldsymbol{x}$ is the origin vertex of the minimum cost path, $\boldsymbol{x}_m = \boldsymbol{y}$ is the destination vertex and m is the number of the optimum path segments.

For color images the connection costs are calculated using the Euclidean distance in RGB color space between neighboring pixels. Thus, the structure of filter output is the same as in the case of the bilateral filter.

4 Experimental Results

In this section we compare the bilateral filter with the proposed modification in terms of the visual quality of the restored image and also in terms of objective quality measures. Additionally, we evaluate the proposed filter efficiency with the denoising methods described briefly in the introduction.

(a) LENA (b) GOLDHILL (c) PEPPERS

Figure 6: Color test images.

First, the relationship between the control parameters of the filters and the noise level was analyzed. The effectiveness of the new filter was tested on the standard color test images LENA, PEPPERS and GOLDHILL (see Fig. 6) corrupted with Gaussian and mixed Gaussian and impulse noise (salt & pepper in each channel). The test images were contaminated by: Gaussian noise of $\sigma = 10$, $\sigma = 20$, $\sigma = 30$, and mixed Gaussian and impulsive noise of $\sigma = 10$ and $p = 0.1$, $\sigma = 20$ and $p = 0.2$, $\sigma = 30$ and $p = 0.3$, where p denotes the contamination probability.

The noise removal capabilities of the modified bilateral filter were extensively tested. To quantitatively evaluate the denoising methods we used the Peak Signal to Noise Ratio (PSNR) and the Mean Absolute Error (MAE) [4].

The Peak Signal to Noise Ratio is defined as

$$PSNR = 20 \log_{10} \left(\frac{255}{\sqrt{MSE}} \right), \qquad (10)$$

where MSE (Mean Squared Error) is given by

$$MSE = \frac{\sum_{i=1}^{N} \sum_{k=1}^{3} [O_k(\boldsymbol{x}_i) - J_k(\boldsymbol{x}_i)]^2}{3N}, \qquad (11)$$

where index k denotes k-th color channel of the pixel, $\boldsymbol{J}(\boldsymbol{x}_i)$ is the pixel of the restored image indexed with i, which indicates its position on the image domain, $\boldsymbol{O}(\boldsymbol{x}_i)$ is the pixel of the original image and N is the total number of image pixels. The PSNR quality measure is used to evaluate the impulsive noise suppression efficiency of a a given filtering solution.

The mean absolute error is defined as

$$MAE = \frac{\sum_{i=1}^{N} \sum_{k=1}^{3} |O_k(\boldsymbol{x}_i) - J_k(\boldsymbol{x}_i)|}{3N}, \qquad (12)$$

and is an indicator of the filter's capability to preserve fine image details.

As can be derived from (4) the properties of the bilateral filter are controlled by the parameters σ_S and σ_I. Figures 7 and 8 show the dependence of the PSNR on the σ_I and σ_S values for the noisy images restored by the bilateral filter with 5×5 and 9×9 filtering windows.

The values of PSNR depend significantly on the σ_I and σ_S parameters. Examining the plots, it can be observed that the optimal value of σ_S is relatively insensitive to noise level in the case of mixed noise but has to be tuned when restoring images polluted by Gaussian noise.

The color images contaminated by mixed Gaussian and impulsive noise were also restored by the modified bilateral filter. This filter was applied for different values of the parameters h in (8) and the dependence of PSNR measure on the parameter h is depicted in Fig. 10.

As can be observed, for test images contaminated by Gaussian noise of increasing intensity, the optimal results depend significantly on the tuning parameter h which increases with the noise magnitude. The obtained results show that the optimal h parameter does not depend significantly on the image structure and the contamination level of the mixed Gaussian and impulsive noise. For images contaminated with this kind of noise the range of the h parameter, for which the optimal PSNR values can be obtained, is $[150, 250]$ and the setting $h = 200$ can be recommended as a default value.

The effectiveness of the new filtering design was compared with several existing methods, described in the Introduction. The first method taken for comparisons is the *Non-Local Means* filter (NLM). The control parameters depend on the noise intensity and were selected experimentally to obtain the best possible results in terms of the PSNR. The second chosen method used for the evaluation of the proposed filter efficiency is the *Anisotropic Diffusion* (AD) implemented with the Gaussian conductivity function [22] and performing as many iterations as required to achieve the maximum PSNR value. Additionally, the efficiency of the new algorithm was compared with the Vector Median Filter (VMF) [12].

The *Bilateral Filter* (BF) and the proposed *Modified Bilateral Filter* (MBF) were tested for windows of size 5×5 and 9×9. The control parameters were selected experimentally to obtain optimal results in terms of the PSNR measure. The comparison of the efficiency of the proposed MBF with the mentioned above filters in terms of

Table 1: Comparison of PSNR (a) and MAE (b) values obtained when restoring the color test images with the proposed algorithm and other denoising techniques.

(a) PSNR

IMAGE	NOISE	METHOD						
		NLM	AD	VMF	$BF_{5\times5}$	$MBF_{5\times5}$	$BF_{9\times9}$	$MBF_{9\times9}$
LENA	σ=10	**34.76**	33.47	27.09	32.86	32.26	32.92	31.93
	σ=20	**31.93**	30.44	26.53	29.38	29.78	29.68	29.48
	σ=30	**30.39**	28.71	25.84	27.27	28.06	27.90	27.98
	σ=10, p=0.1	19.51	25.24	26.75	27.50	**28.28**	**28.27**	27.48
	σ=20, p=0.2	20.22	24.01	25.15	24.81	**26.41**	26.221	**26.89**
	σ=30, p=0.3	21.09	22.67	23.11	22.66	**24.55**	24.34	**25.98**
GOLDHILL	σ=10	**33.40**	32.11	25.31	31.90	30.91	31.90	30.74
	σ=20	**30.21**	29.02	24.94	28.56	28.30	28.74	27.98
	σ=30	**28.19**	27.41	24.47	26.47	26.79	26.84	26.55
	σ=10, p=0.1	17.92	24.03	25.00	25.52	**25.99**	**26.16**	25.13
	σ=20, p=0.2	19.68	23.29	23.92	23.91	**24.95**	25.06	**25.15**
	σ=30, p=0.3	20.63	22.05	22.29	21.97	**23.50**	23.51	**24.70**
PEPPERS	σ=10	**33.71**	33.03	26.54	32.15	31.74	32.29	31.55
	σ=20	**31.31**	30.19	25.97	28.73	29.51	28.92	29.39
	σ=30	**29.81**	28.40	25,27	26.70	27.61	27.13	27.75
	σ=10, p=0.1	18.54	24.33	26.01	26.37	**26.95**	**27.07**	26.46
	σ=20, p=0.2	19.48	22.52	24.50	23.46	**24.87**	24.69	**25.61**
	σ=30, p=0.3	19.68	20.83	22.96	21.18	**22.82**	22.57	**24.37**

(b) MAE

IMAGE	NOISE	METHOD						
		NLM	AD	VMF	$BF_{5\times5}$	$MBF_{5\times5}$	$BF_{9\times9}$	$MBF_{9\times9}$
LENA	σ=10	**3.53**	4.07	6.71	4.42	4.51	4.35	4.71
	σ=20	**4.79**	5.66	7.58	6.69	6.02	6.39	5.99
	σ=30	**5.53**	6.85	8.56	8.35	7.50	7.44	7.18
	σ=10, p=0.1	9.22	9.16	7.09	7.36	**6.45**	6.55	**6.64**
	σ=20, p=0.2	11.76	11.42	8.90	10.66	**8.52**	8.91	**7.54**
	σ=30, p=0.3	13.93	14.43	11.36	14.16	**11.12**	11.36	**8.99**
GOLDHILL	σ=10	**4.20**	4.87	9.20	5.02	5.51	5.00	5.57
	σ=20	**5.99**	8.19	9.94	7.35	7.33	7.16	7.51
	σ=30	**7.41**	4.87	10.71	9.22	8.78	9.00	8.82
	σ=10, p=0.1	13.24	12.07	9.50	9.67	**9.03**	**8.97**	9.81
	σ=20, p=0.2	13.80	13.51	10.96	12.06	**10.44**	10.55	**9.97**
	σ=30, p=0.3	16.06	16.00	12.95	15.50	**12.63**	13.02	**10.77**
PEPPERS	σ=10	**3.98**	4.41	6.80	4.90	4.91	4.81	4.94
	σ=20	**5.13**	5.92	7.70	7.05	6.38	6.59	6.24
	σ=30	**5.84**	7.25	8.68	8.88	7.98	8.16	7.51
	σ=10, p=0.1	10.49	10.69	7.18	8.24	**7.20**	7.42	**7.30**
	σ=20, p=0.2	13.21	14.22	9.06	12.30	**9.76**	10.48	**8.52**
	σ=30, p=0.3	16.59	18.06	11.50	16.68	**13.35**	14.08	**10.54**

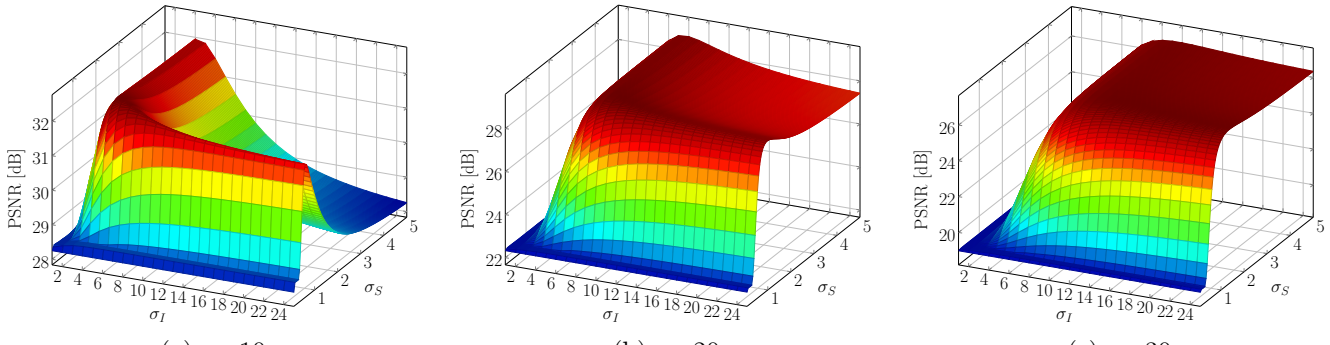

(a) σ=10 (b) σ=20 (c) σ=30

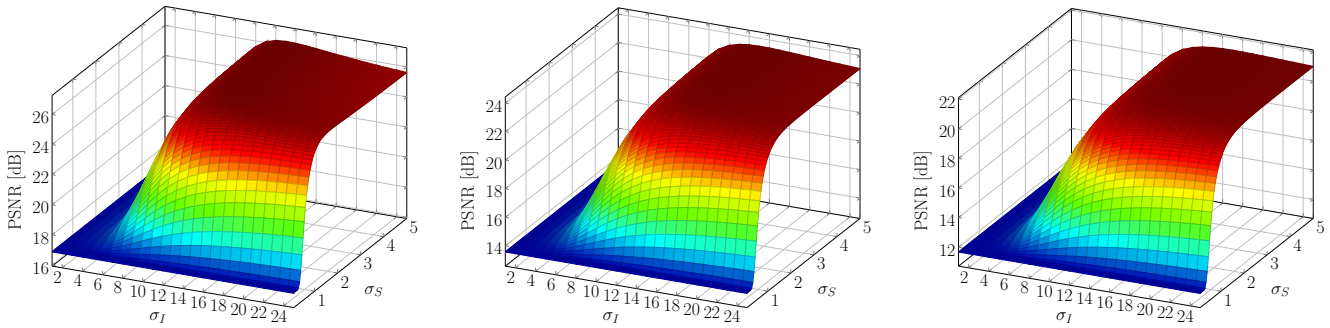

(d) σ=10, p=0.1 (e) σ=20, p=0.2 (f) σ=30, p=0.3

Figure 7: Dependence of PSNR on σ_S and σ_I parameters for the bilateral filter operating on 5×5 window). The test color image PEPPERS color image was corrupted by Gaussian (a, b, c) and mixed Gaussian and impulse noise (d, e, f)

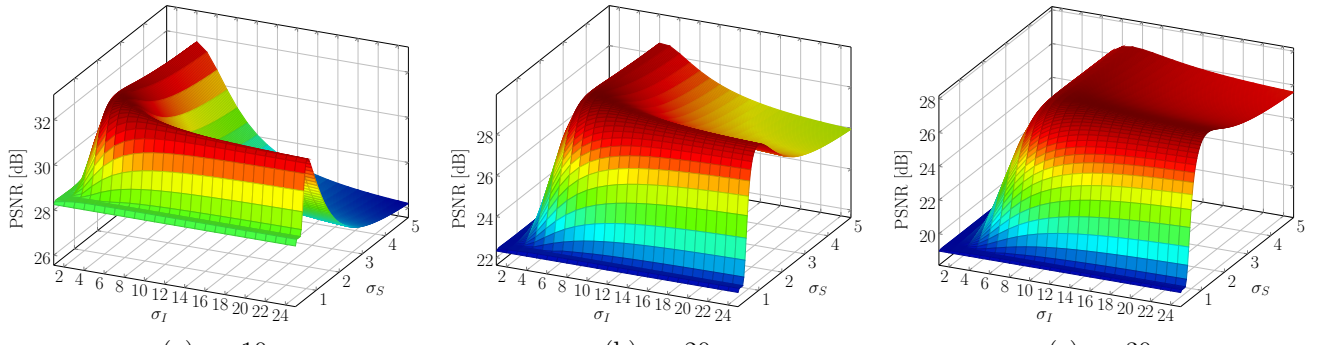

(a) σ=10 (b) σ=20 (c) σ=30

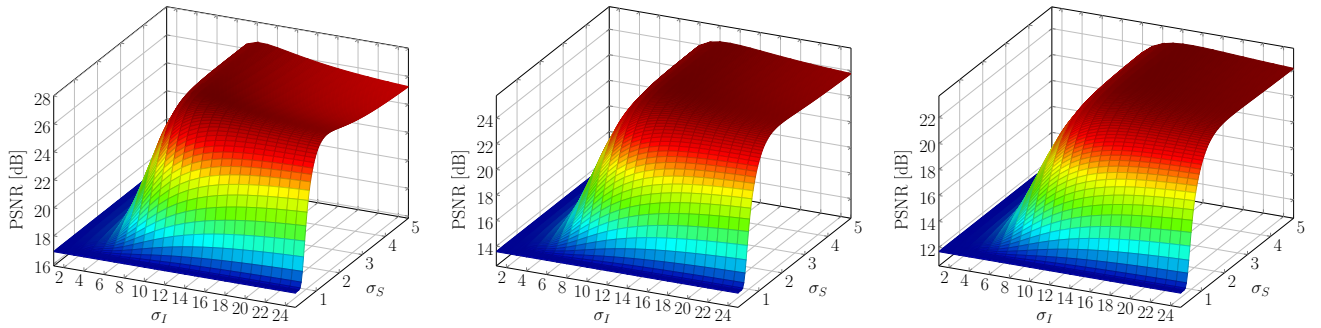

(d) σ=10, p=0.1 (e) σ=20, p=0.2 (f) σ=30, p=0.3

Figure 8: Dependence of PSNR on σ_S and σ_I parameters for the bilateral filter operating in 9×9 window. The color image PEPPERS was corrupted by Gaussian (a, b, c) and mixed Gaussian and impulse noise (d, e, f).

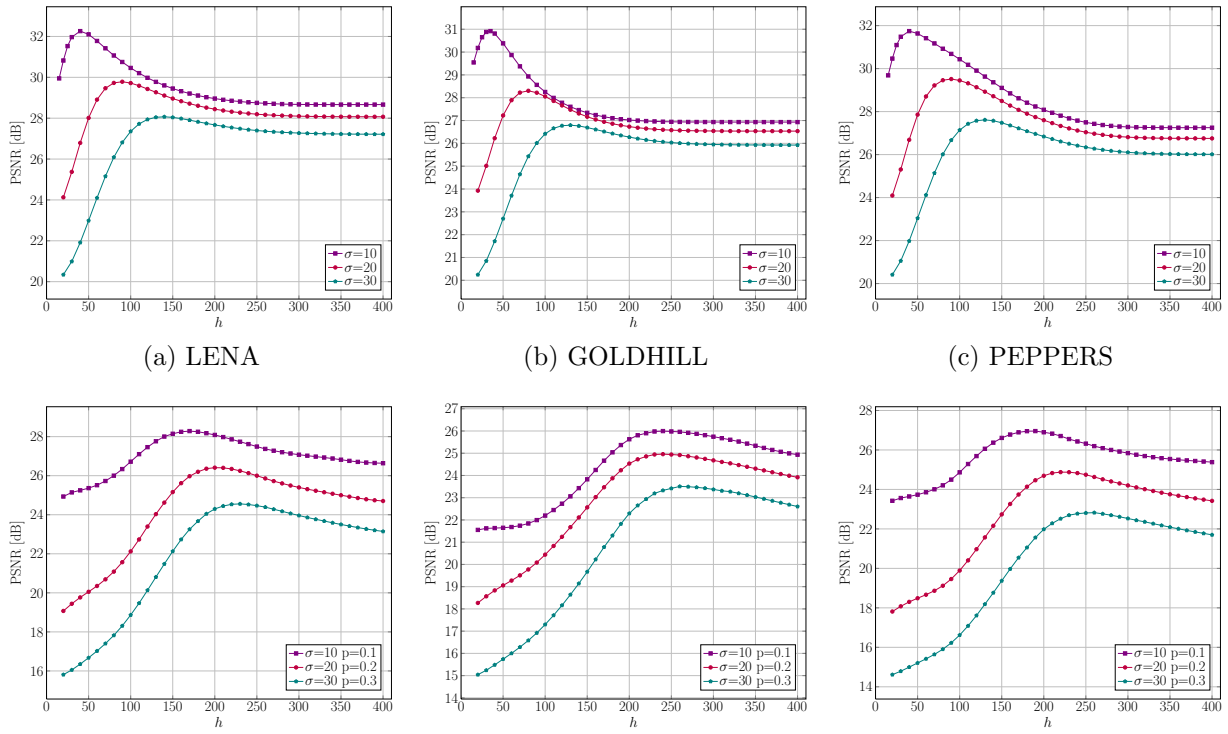

(a) LENA (b) GOLDHILL (c) PEPPERS

(d) LENA (e) GOLDHILL (f) PEPPERS

Figure 9: Dependence of PSNR when applying the modified bilateral filter using a 5×5 window on the h parameter for the color image PEPPERS corrupted with Gaussian (a, b, c) and mixed Gaussian and impulse noise (d, e, f).

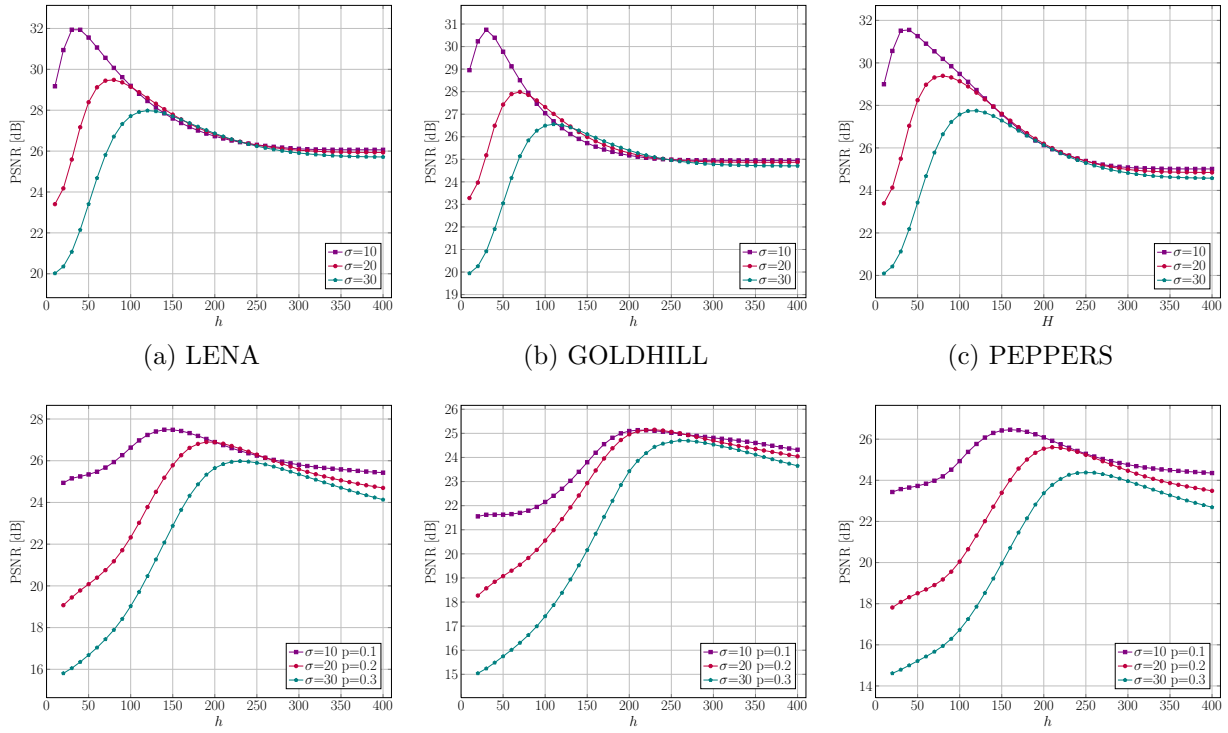

(a) LENA (b) GOLDHILL (c) PEPPERS

(d) LENA (e) GOLDHILL (f) PEPPERS

Figure 10: Dependence of PSNR when applying the modified bilateral filter using a 9×9 window on the h parameter for the color image PEPPERS corrupted with Gaussian (a, b, c) and mixed Gaussian and impulse noise (d, e, f).

(a) (b) (c)

(d) (e) (f)

Figure 11: Comparison of the efficiency of the bilateral filter with the proposed approach: (a) PEPPERS image corrupted by mixed noise (σ=20, p=0.2), (b) BF output , (c) MBF output, (d) PEPPERS image corrupted by mixed noise (σ=30, p=0.3), (e) BF output, (f) MBF output, (filtering window 5×5).

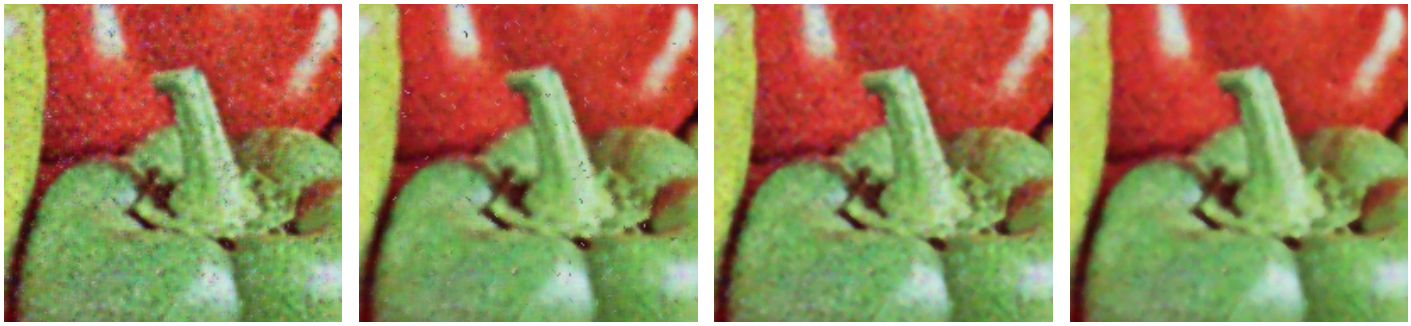

(a) PSNR=23.5 dB (b) PSNR=24.9 dB (c) PSNR=24.2 dB (d) PSNR=25.7 dB

Figure 12: Results of the restoration of the test color image PEPPERS corrupted by mixed noise (σ=20, p=0.2) using a 5×5 filtering window: (a) BF output , (b) MBF output, (c) BF with additional denoising of impulses using the method described in [18], (d) MBF with the same impulsive noise removal technique.

(a) noisy image (b) BF (c) MBF

Figure 13: Illustration of the efficiency of the modified bilateral filter (MBF) in comparison with the standard version (BF).

PSNR and MAE are summarized in Tab. 1.

As can be observed, for images contaminated by Gaussian noise, the best results are obtained by the NLM algorithm and the results of the modified bilateral are quite similar to those obtained using the bilateral filter. However, the results for images contaminated by mixed Gaussian and impulse noise obtained using the new filter are significantly better, especially for images contaminated by high and medium mixed noise levels.

Figure 11 exhibits the restoration results of the modified and standard bilateral filter. As can be observed using the proposed modification the edges and details are better preserved and the filtering output is visually more pleasing. Unfortunately, as can be noticed in the images contaminated by a mixed Gaussian and impulse noise, small clusters consisting of two or more pixels distorted by impulsive noise are beeing preserved. However, for images processed with the modified bilateral, this artifact can be easily removed using a switching filter with good impulse detection mechanism [9, 33].

For images processed with the standard bilateral filter, the removal of the remaining impulse noise is more difficult, because the impulses are blurred by the image restoration technique. The restoration results with additional impulsive noise reduction, using the method described in [18], are presented in Fig. 12.

The high efficiency of the proposed approach is also confirmed by Fig. 13 which depicts the restoration results of a noisy image acquired using a high speed camera under poor lighting conditions. As can be observed, the noise is better suppressed and the edges are well preserved.

5 Conclusions

In the paper a novel filtering scheme has been proposed and analyzed. The results of the performed experiment indicate that very good restoration quality has been achieved for color images contaminated by strong mixed Gaussian and impulsive noise. The new filtering method yields significantly better results in comparison with other denoising schemes both in terms of subjective image quality and objective restoration measures. The beneficial feature of the proposed method is the removal of mixed noise and the ability to preserve image edges and fine details. In the future work, we want to study the influence of the definition of connection cost function and the choice of the weighting function on the image restoration results. We also plan to investigate the efficiency of the proposed design with incorporated spatial distance parameter which penalizes long paths exploring the local filtering window.

Acknowledgement

This work has been supported by the Polish Ministry of Science and Higher Education Development Grant OR 00002111.

References

[1] Boncelet, C.G.: Image noise models. In Bovik, A.C. editor, Handbook of Image and Video Processing, Communications, Networking and Multimedia, 397–410. Elsevier Academic Press, (2005).

[2] Zheng, J., Valavanis, K.P., Gauch, J.M.: Noise removal from color images. Journal of Intelligent and Robotic Systems 7(3), 257–285, (1993).

[3] Lukac, R., Smolka, B., Martin, K., Plataniotis, K.N., Venetsanopoulos, A.N.: Vector filtering for color imaging. IEEE Signal Processing Magazine, 22(1), 74–86, (2005).

[4] Plataniotis, K.N., Venetsanopoulos, A.N.: Color Image Processing and Applications, Springer, (2000).

[5] Peng, S., Lucke, L.: Multi-level adaptive fuzzy filter for mixed noise removal. In IEEE International Symposium on Circuits and Systems, 2, 1524 –1527, (1995).

[6] Wang, C., Yang, B. Sun, L.-F., Liu, Y.-M., Yang, S.-Q.: Video enhancement using adaptive spatio-temporal connective filter and piecewise mapping. EURASIP J. Adv. Sig. Proc. 2008, (2008).

[7] Garnett, R., Huegerich, T., Chui, C., Wenjie, H.: A universal noise removal algorithm with an impulse detector. IEEE Transactions on Image Processing 14(11), 1747–1754, (2005).

[8] Tang, K., Astola, J., Neuvo, Y.: Nonlinear multivariate image filtering techniques. IEEE Transactions on Image Processing 4(6), 788–798, (1995).

[9] Lukac R.: Adaptive vector median filtering. Pattern Recognition Letters 24(12), 1889–1899, (2003).

[10] Lukac, R., Smolka, B., Plataniotis, K.N., Venetsanopoulos, A.N.. Vector sigma filters for noise detection and removal in color images. Journal of Visual Communication and Image Representation 17(1), 1–26, (2006).

[11] Pitas, I., Tsakalides, P.: Multivariate ordering in color image filtering. IEEE Transactions on Circuits and Systems for Video Technology 1(3), 247–259, 295–6, (1991).

[12] Astola, J., Haavisto, P., Neuvo, Y.: Vector median filters. Proceedings of the IEEE 78(4), 678–689, (1990).

[13] Plataniotis, K.N., Androutsos, D., Venetsanopoulos, A.N.: Multichannel filters for image processing. Signal Processing: Image Communication 9(2), 143–158, (1997).

[14] Plataniotis K.N., Androutsos, D., Vinayagamoorthy, S., Venetsanopoulos, A.N.: An adaptive nearest neighbor multichannel filter. IEEE Trans. on Circuits and Systems for Video Technology 6(6), 699–703, (1996).

[15] Lukac, R., Plataniotis, K.N., Venetsanopoulos, A.N., Smolka, B.: A statistically-switched adaptive vector median filter. Journal of Intelligent and Robotic Systems 42(4), 361–391, (2005).

[16] Kenney, C., Deng, Y., Manjunath, B. S., Hewer G.: Peer group image enhancement. IEEE Transactions on Image Processing 10(2), 326–334, (2001).

[17] Deng, Y., Kenney, C., Moore, M.S., Manjunath, B.S.: Peer group filtering and perceptual color image quantization. In Proceedings of the 1999 IEEE International Symposium on Circuits and Systems, 4, 21–24, (1999).

[18] Smolka, B., Chydzinski, A.: Fast detection and impulsive noise removal in color images. Real-Time Imaging 11(5-6), 389–402, (2005).

[19] Smolka, B.: Peer group switching filter for impulse noise reduction in color images. Pattern Recognition Letters 31(6), 484–495, (2010).

[20] Morillas, S., Gregori, V., Peris-Fajarneés, G., Sapena A.: New adaptive vector filter using fuzzy metrics. Journal of Electronic Imaging 16(3), 033007, (2007).

[21] Morillas, S., Gregori, V., Hervas, A.: Fuzzy peer groups for reducing mixed Gaussian-impulse noise from color images. IEEE Transactions on Image Processing 18(7), 1452–1466, (2009).

[22] Perona, P., Malik, J.: Scale-space and edge detection using anisotropic diffusion. IEEE Transactions on Pattern Analysis and Machine Intelligence 12(7), 629–639, (1990).

[23] Sapiro, G., Ringach, D.L.: Anisotropic diffusion of multivalued images with applications to color filtering. IEEE Trans. on Image Processing 5(11), 1582–1586, (1996).

[24] Gerig, G., Kubler, O., Kikinis, R., Jolesz, F.A.: Nonlinear anisotropic filtering of MRI data. IEEE Transactions on Medical Imaging 11(2), 221–232, (1992).

[25] Buades, A., Coll, B., Morel, J.M.: A non-local algorithm for image denoising. In IEEE Conf. on Computer Vision and Pattern Recognition 2, 60–65, Washington, DC, USA, (2005).

[26] Buades, A., Coll, B., Morel, J.M.: A review of image denoising algorithms, with a new one. Multiscale Modeling and Simulation 4(2), 2006.

[27] Tomasi, C., Manduchi, R.: Bilateral filtering for gray and color images. In Proceedings of the IEEE Int. Conf. on Computer Vision 839–846, 1998.

[28] Paris, S., Durand, F.: A fast approximation of the bilateral filter using a signal processing approach. Int. J. Comput. Vision 81(1), 24–52, 2009.

[29] Barash, D.: Fundamental relationship between bilateral filtering, adaptive smoothing, and the nonlinear diffusion equation. IEEE Transactions on Pattern Analysis and Machine Intelligence 24(6), 844–847, 2002.

[30] Elad, M.: On the origin of the bilateral filter and ways to improve it. IEEE Transactions on Image Processing 11(10), 1141–1151, (2002).

[31] Dijkstra, E.W.: A note on two problems in connexion with graphs. Numerische Mathematik 1, 269–271, (1959).

[32] Falcao, A.X., Stolfi, J., de Alencar Lotufo, R.: The image foresting transform: theory, algorithms, and applications. IEEE Transactions on Pattern Analysis and Machine Intelligence 26(1), (2004).

[33] Smolka, B., Plataniotis, K.N., Chydzinski, A., Szczepanski, M., Venetsanopoulos, A.N., Wojciechowski, K.: Self-adaptive algorithm of impulsive noise reduction in color images. Pattern Recognition 35(8), 1771–1784, (2002).